Discover Nano

RESEARCH Open Access

The refractive index of silver nanowire networks: a heuristic approach to the foundations of the optical constants, from experiment to theory

Amaury Baret[1*], Julia Baumgarten[1,2], François Balty[1,2], Frédéric Rabecki[3], Jérémy Brisbois[3], Buyun Zheng[4], Daniel Bellet[4] and Ngoc Duy Nguyen[1]

*Correspondence:
Amaury Baret
abaret@uliege.be
[1]SPIN, Department of Physics, University of Liège, Allée du Six Août, Liège 4000, Belgium
[2]EPNM, Department of Physics, University of Liège, Allée du Six Août, Liège 4000, Belgium
[3]STAR, Centre Spatial de Liège, Avenue du Pré Aily, Liège 4031, Belgium
[4]Univ. Grenoble Alpes, CNRS, Grenoble INP, LMGP, Grenoble 38000, France

Abstract
This study employs Mie's scattering theory and van de Hulst's mixing model to predict the refractive indices (n, k) of silver nanowire (AgNW) networks in the visible and near-infrared wavelengths, allowing the comparison to the experimentally determined k spectra. Transmittance spectra calculated via the numerical resolution of Fresnel's equations are compared to experimental data, showing excellent agreement, particularly for nanowires with larger diameters and at shorter wavelengths. These findings, both theoretical and empirical, pave the way for accurate optical simulations of metallic nanowire networks, supporting their integration into complex multilayer systems and devices such as displays or smart windows. Notably, our work proposes the first demonstration of the dominance of the metallic character of AgNW networks over their dielectric behavior in terms of optical response.

Keywords Refractive indices, Mie theory, Silver nanowire networks

1 Introduction

Transparent Conducting Materials (TCMs) constitute an essential class of materials that combine high optical transparency with excellent electrical conductivity, making them key building blocks of most modern electronic devices such as photovoltaic cells, OLEDs, transparent heaters, sensors or smart windows [1, 2]. Indium Tin Oxide (ITO) remains the most widely used TCM due to its excellent optoelectronic properties [3], but extensive research for alternatives has been carried out over the past decade, motivated by the limited supply of ITO, its known brittleness and stringent deposition temperatures [4]. Amongst these alternatives, AgNW networks stand out as one of the most promising candidates thanks to their optical transparency and sheet resistance comparable to those of ITO (sheet resistance of a few $\Omega.\,\mathrm{sq}^{-1}$ associated with an optical transmittance of 80% at the wavelength $\lambda = 550$ nm), with the added benefits of high mechanical

flexibility, as well as low-cost and scalable deposition methods [5, 6]. While the use of AgNW networks does present challenges, such as surface roughness and susceptibility to environmental degradation, these can be effectively mitigated through protective coatings based on semiconducting oxides such as ZnO or SnO_2 [7–10]. The electrical conductivity of silver nanowire networks originates from a percolation mechanism, through which current can flow via the intersections between nanowires [11–15]. The optical transparency is made possible by the remaining gaps in between the nanowires, allowing light to go through. Both properties are connected to one another, as adding more nanowires tends to increase the conductance while decreasing the transmittance, and inversely [16]. This trade-off is well-known and when designing networks for applications, its optimum, typically quantified via Haacke's figure of merit [17], is application-dependent [18]. In that context, being able to predict the optical properties of the AgNW network holds much importance. When studying a material's optical properties, determining its refractive indices (RIs) is often insightful. The knowledge - and physical understanding - of the RIs of a material serves as a physical probe into its fundamental optical properties. Additionally, it enables the material's integration into multilayer stack simulations, commonly performed with the Transfer Matrix Method (TMM) [19–21]. This method allows for the calculation of the optical transmittance, reflectance, and absorbance of a stack, provided the RIs of all constituent materials are known across relevant wavelengths, thus facilitating the design of complex devices that combine multiple materials such as those typically used in smart windows [22] or solar cell designs [23].

Determining the refractive indices (RIs) of silver nanowire (AgNW) networks, whether experimentally or theoretically, is challenging. Existing empirical protocols are generally unsuitable for AgNW networks due to their high inhomogeneity and lack of interference at the substrate interface. In past studies on the RIs of AgNW networks, such as those from Yu et al. [24] or Abdel-Rahim et al. [25], one method is predominantly used: measuring the total optical transmittance T and reflectance R with a spectrophotometer under normal incidence, from which the complex refractive index $\tilde{n} = n + ik$ is extracted. A notable exception to that approach lies in the work of Tomiyama et al., who used spectroscopic ellipsometry to deduce the optical constants of a polymer-embedded AgNW network [26]. Concerning the former method, the imaginary coefficient k is determined through Beer-Lambert's law,[1] reasonably assuming normal incidence and that the material's thickness d corresponds in first approximation to the nanowires' average diameter [27]:

$$k = \frac{\lambda}{4\pi d} \ln\left(\frac{1-R}{T}\right) \tag{1}$$

which relates the total absorption A to the film's thickness d. The real part of the refractive index, n, is then calculated from T and R using [28, 29]:

$$n = \frac{1+R}{1-R} + \sqrt{\frac{4R}{(1-R)^2} - k^2}. \tag{2}$$

[1] In the case of the imaginary RI k and given a non-absorbing substrate such as glass one can only consider the AgNW network and not the effect of the substrate.

In this work, we argue that Eq. (2) yields only the *effective* refractive indices of the (AgNW network/glass) hybrid, rather than those of the AgNW network alone. This argument stems from the observation that Eq. (2) is traditionally applied to isotropic, homogeneous dielectric materials with smooth boundaries [28–30], conditions which do not describe the heterogeneous, metallic-dielectric nature of AgNW networks. The latter indeed exhibit characteristics of both metals and dielectrics - electrical conductivity and optical transparency -, such that assuming that they follow a purely dielectric optical behavior would require a solid theoretical or experimental validation. Furthermore, the structure of Eq. (2) inherently constrains the value of n to be equal to or greater than 1, which is incompatible with metallic materials deposited on dielectrics, as these typically exhibit n values below 1 in the visible range due to surface plasmon resonance effects arising from free electron oscillations [31].

2 Methods

In light of the aforementioned observations and as illustrated in Fig. 1, we propose an original approach to investigate the RIs of AgNW networks. We do however note that the determination of the *effective* refractive index remains useful, as it can allow for the prediction of the optical behavior of the combined (AgNW network/glass) hybrid material, making it valuable for applications in which that specific hybrid's optical response is of primary interest. Further development on that aspect can be found in S2 of the Supplementary Information.

In this work, our approach consists in the theoretical prediction of the RIs of AgNW networks themselves using a combination of the Mie and van de Hulst (vdH) models, rather than in their experimental determination. Both are fundamental models free of any fitting parameter and, when used together, allow for the prediction of the far-field optical response of well-defined nanostructures embedded in transparent dielectrics. Considering the nanowires as cylinders, for which analytical solutions can be found by application of Mie's theory, Manning et al. and Hamans et al. predicted the transmittance of such networks at $\lambda = 550$ nm [32, 33] based on original research by Khanarian et al. [34]. However, Mie's theory alone does not suffice for the determination of the

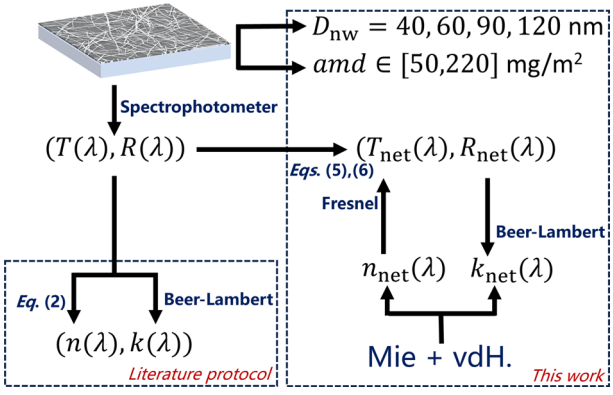

Fig. 1 Schematic summary of the research undertaken in this work. The optical transmittance and reflectance of AgNW samples of varying average diameters and areal mass densities were measured via a spectrophotometer under normal incidence. The existing protocol typically used in the literature consists in using Eqs. (1) and (2) to determine the RIs of the (network/glass hybrid). In this work, we focused on extracting the RIs of the network themselves by using a combination of the theoretical Mie and vdH models. Fresnel and Beer-Lambert laws allow for the verification of the models predictions

RIs of the network. To bridge that gap, Khanarian et al. pioneered the use of the vdH model for the description of AgNW networks embedded in a polymer matrix. Despite the use of cylindrical nanowires in the model rather than pentagonal [35, 36], Khanarian et al. showed the good agreement between the theoretical prediction of the 'Mie + vdH' model and the optical response of AgNW networks embedded in a transparent polymer matrix over visible wavelengths. The present research aims to generalize the results of Khanarian et al. by predicting the *n* values of a AgNW network in air - its most general form -, in order to test further the validity of these combined models. Furthermore, we explore a larger interval of wavelengths, spanning from the early visible to the NIR, such that the limits of the model can be determined and that the results can be exploited for many types of applications that are not restricted to the visible spectrum. Finally, we also study the impact of the average nanowire diameter and of the network's density, described in this article through the areal mass density (*amd*), on the predictions of such models. Both *n* and *k* can be predicted using this model, but only the values of *k* can be compared to the experimentally determined ones due to the reasons previously detailed. Consequently, in order to test the predicted values of *n*, Fresnel's equations were used to calculate the transmittance of the network based on the Mie-determined sets of (*n*, *k*) and compare it to the experimentally measured ones. A schematic summary of our approach can be found in Fig. 1, highlighting the key steps in our description of the optical properties of AgNW networks.

Mie's theory provides a rigorous solution to Maxwell's equations for the scattering and absorption of electromagnetic waves by infinitely long cylindrical particles, to which nanowires can be reasonably compared. While the pentagonal geometry of AgNWs may impact local field distributions, the cylindrical approximation remains sufficient to capture the far-field optical behavior of the networks, as validated by the strong agreement between modeled and measured spectra by Khanarian et al. Specifically, Mie theory enables the computation of the scattering efficiencies of individual AgNWs (thus assumed as cylinders) as a function of their dimensions D_{NW} and L_{NW}, the wavelength λ, and the RIs of silver. The scattering amplitude under normal incidence $S(\theta = 0)$ is given by [34]:

$$S(0) =< S_s(0) + S_p(0) >= 0.5 \times \left[a_0 + 2\sum_{n=1}^{\infty} a_n + b_0 + 2\sum_{n=1}^{\infty} b_n\right], \tag{3}$$

where a_n and b_n are the Mie coefficients associated with the scattering of light onto the cylinder and whose expressions can be found in most optical reference books [37], and S_s, S_p correspond to the scattering amplitudes of *s* and *p*-polarized incident light, respectively (more details can be found in Supplementary Information S3). The vdH mixing model extends the applicability of the Mie's solution to heterogeneous media, allowing us to describe the effective refractive index of a composite material comprising AgNWs embedded in a matrix of air [38]. The model combines the contributions of the individual nanowires weighted by their volumetric fraction f_v and spatial arrangement (assuming a homogeneous and isotropic distribution of the nanowires), effectively bridging the microscopic Mie scattering results with macroscopic optical behavior. Based on that model, the effective composite refractive indices are:

$$n_{\text{net}}(\lambda) = n_{\text{air}}(\lambda)\left(1 + \frac{f_v\lambda^2}{2\pi^2 c D_{\text{NW}}^2}\,\text{Im}[S(0)]\right),$$
$$k_{\text{net}}(\lambda) = n_{\text{air}}(\lambda)\frac{f_v\lambda^2}{2\pi^2 c D_{\text{NW}}^2}\,\text{Re}[S(0)],$$

where $c = 0.617$ is a dimensionless geometrical factor relating the volume of a nanowire to its projected area (See Supplementary Information S1 for more details). In summary, this hybrid approach offers a physically grounded framework for modeling the complex and heterogeneous nature of AgNW networks by treating them as an equivalent smooth thin film system of air in which nanowires are stochastically embedded. With the refractive indices (*n*, *k*) predicted by the Mie+vdH model, we calculate the transmittance T_{net} of the networks using the Fresnel's and Beer-Lambert's equations. The former equation describes the interaction of light with interfaces between materials of differing refractive indices:

$$R(\lambda) = \frac{(1 - n(\lambda))^2 + k^2(\lambda)}{(1 + n(\lambda))^2 + k^2(\lambda)} \tag{4}$$

From there, the well-known identity $T(\lambda) = 1 - A(\lambda) - R(\lambda)$ can be used to deduce the value of *T*. We note that the absorbance *A* is not related to the scattering efficiencies that appear in Mie's model but rather strictly quantifies the amount of power absorbed by the AgNW network given its refractive indices.

3 Results and discussion

The measured optical transmittance and reflectance spectra in the visible and near-infrared wavelengths [300–2500] nm of AgNW networks of varying nanowire density and with different average diameters D_{NW} are shown in Fig. 2 (See S1 of the Supplementary Information for more information on experimental methods). The transmittance and reflectance of the network itself, respectively T_{net} and R_{net}, were extracted from the AgNW/glass as follows:

$$T_{\text{net}}(\lambda) = \frac{T(\lambda)}{T_{\text{glass}}(\lambda)} \tag{5}$$

$$R_{\text{net}}(\lambda) = R(\lambda) - R_{\text{glass}}(\lambda) \tag{6}$$

The transmittance of all samples decreases with increasing wavelength, an observation already made and explained by Atkinson et al. [39] as the consequence of the combined effect of *(i)* the increase of the RIs (both *n* and *k*) of silver itself with increasing wavelength, leading to a simultaneous increased absorbance and reflectance of the nanowires themselves, and *(ii)* the average spacing size between the nanowires, which plays an important role in the transmission of light whose wavelengths are comparable or larger than the characteristic dimension of said gaps. These effects also explain the dependence of the rate of the transmittance drop as a function of the wavelength, as thicker diameter NWs tend to have a lower imaginary part of the RI due to lower surface scattering effects, and have higher average spacings than smaller diameter nanowires. From the curves in Fig. 2, Eq. (1) was used to deduce the imaginary coefficient *k* spectra of the networks as a function of the wavelength.

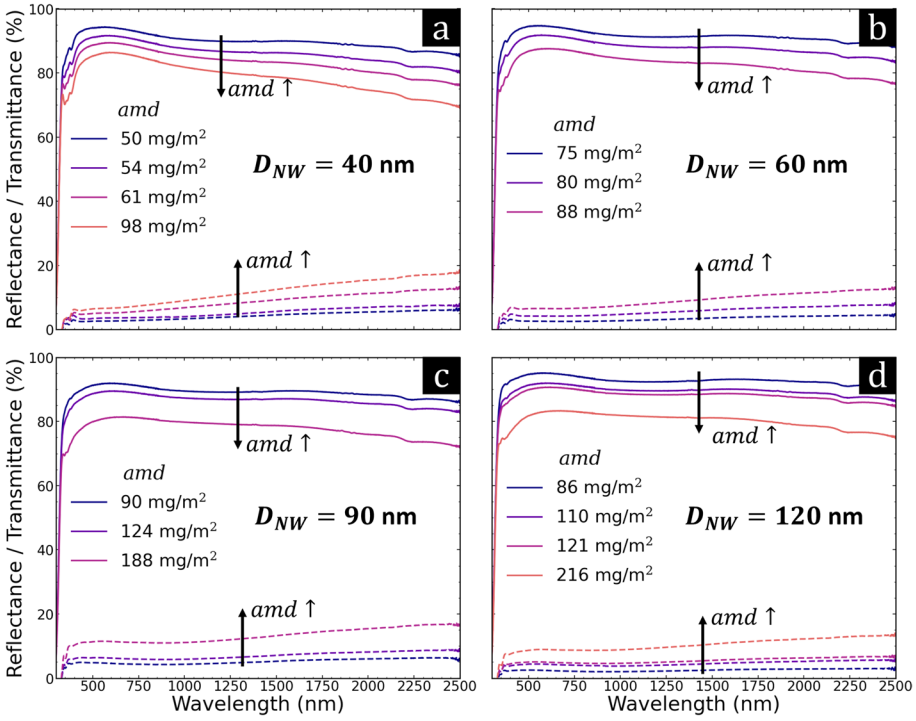

Fig. 2 Optical transmittance (solid lines) and reflectance (dashed lines) of AgNW networks under normal incidence with D_{NW} =**a** 40 nm, **b** 60 nm, **c** 90 nm and **d** 120 nm. For each average diameter, varying densities, expressed in areal mass density (*amd*), were investigated. Note that for a given f_A, the *amd* explicitly depends on D_{NW}, such that thicker NWs networks are associated to higher *amds*, and reciprocally. Due to the low noise associated with the optical measurements, the error bars (of the order of 1 %) are not visible in the plots

Figure 3 presents the empirically deduced k spectra alongside the predicted values obtained from the Mie+vdH model for varying nanowire diameters and densities. A detailed examination reveals a general upward trend of k with increasing wavelength. Notably, the slope of this trend intensifies with smaller nanowire diameters and higher densities. This behavior can be attributed to the intrinsic optical properties of silver, which are well-approximated by Drude's model [40]. The observed increase in k with wavelength reflects the dissipative nature of the free electron response in metals. At longer wavelengths, the interaction of free electrons with the electromagnetic field becomes more significant due to enhanced low-frequency scattering. This scattering is a result of the increasing contribution of Ohmic losses, where longer electron oscillation periods (relative to the plasma frequency of silver, approximately $c/(328\,\mathrm{nm})$ [41]) amplify energy dissipation and absorption. Such mechanisms are characteristic of the longer wavelength ranges explored in this study. The influence of nanowire density on k is also evident. As density increases, the areal filling fraction (f_A) of the network rises, leading to more pronounced metallic behavior [42]. This manifests as higher k values across the spectrum. Similarly, variations in nanowire diameter significantly impact k. Thinner nanowires result in shorter electron mean free paths due to more frequent interactions between free electrons and the nanowire surfaces. This reduction in mean free path enhances energy dissipation, further increasing k.

Figure 4 shows the measured and theoretical transmittance curves, alongside the predicted n values derived using the Mie+vdH model. The gray area corresponds to the model predictions for a 20% variation in input nanowire density, accounting for the

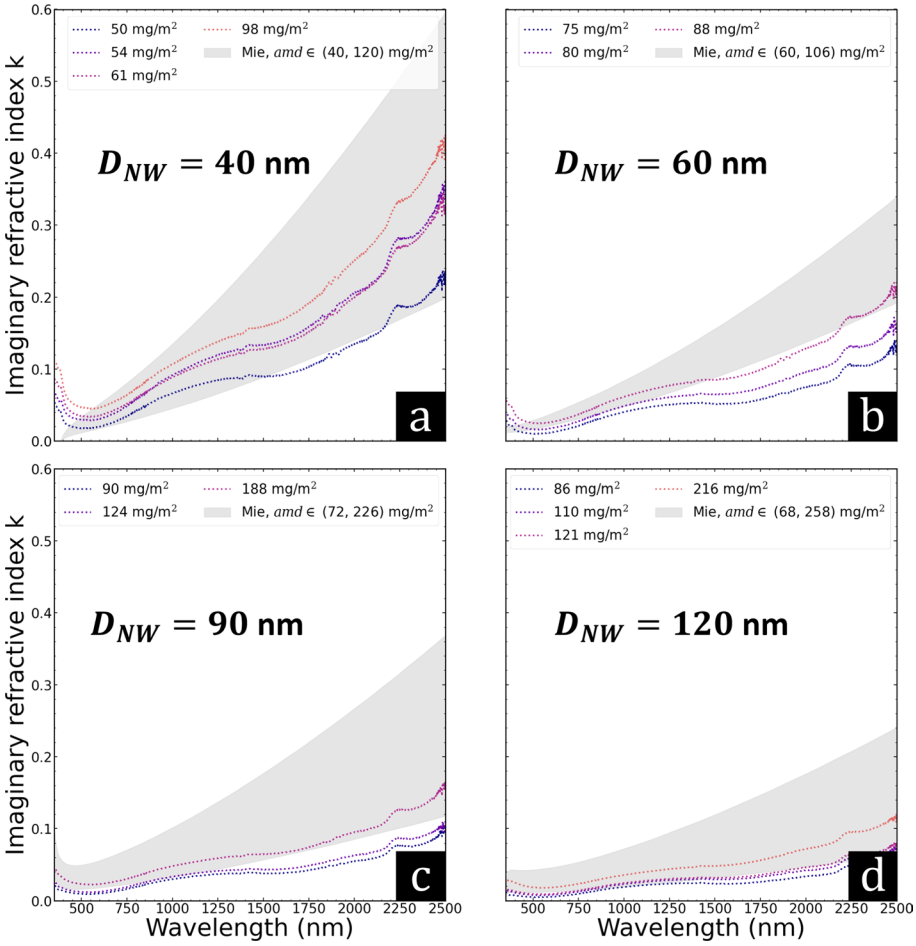

Fig. 3 Imaginary part of the refractive index, *k*, as a function of the wavelength, as determined by Eq. (1) (dashed lines) and as predicted by the Mie+vdH models (gray areas). The latter were calculated for *amd* values spanning the $(amd_{\min} - 20\%, amd_{\max} + 20\%)$ range for each given D_{NW}, such as to account for the intrinsic error associated to the *amd* measurement. Due to the low noise associated with the optical measurements, the horizontal error bars (of the order of 1 %) are not visible in the plots

measurement uncertainty on this parameter. A comparison between the theoretical transmittance of the network (T_{net}) and experimental data demonstrates fair agreement, particularly for networks with larger nanowire diameters (D_{NW}) and at shorter wavelengths. This enhanced matching between theory and experiment is attributed to the greater accuracy of the vdH model at shorter wavelengths relative to the structure size, addressing a known limitation of this theoretical framework. At large wavelengths, when $\lambda/D_{NW} > 25$ (size parameter $\alpha = (\pi R_{NW})/\lambda < 0.06$ where R_{NW} is the radius of the nanowires), deviations are observed between the model and the experimental results. We attribute this breakdown to the limitations of van de Hulst's mixing rule, which assumes independent scattering and relies on the anomalous diffraction approximation (ADT), both of which lose validity when the size parameter becomes small ($\alpha < 0.2$), i.e. when the wavelength of the incident light becomes too large compared to the characteristic size of the nanostructure [38, 43, 44]. This constitutes a limitation to the models, not identified before, and which should be explicitly considered when simulating the optical properties of silver nanowire networks with this theoretical framework. The observed increase in *n* with wavelength is distinctly different from the behavior of metallic thin

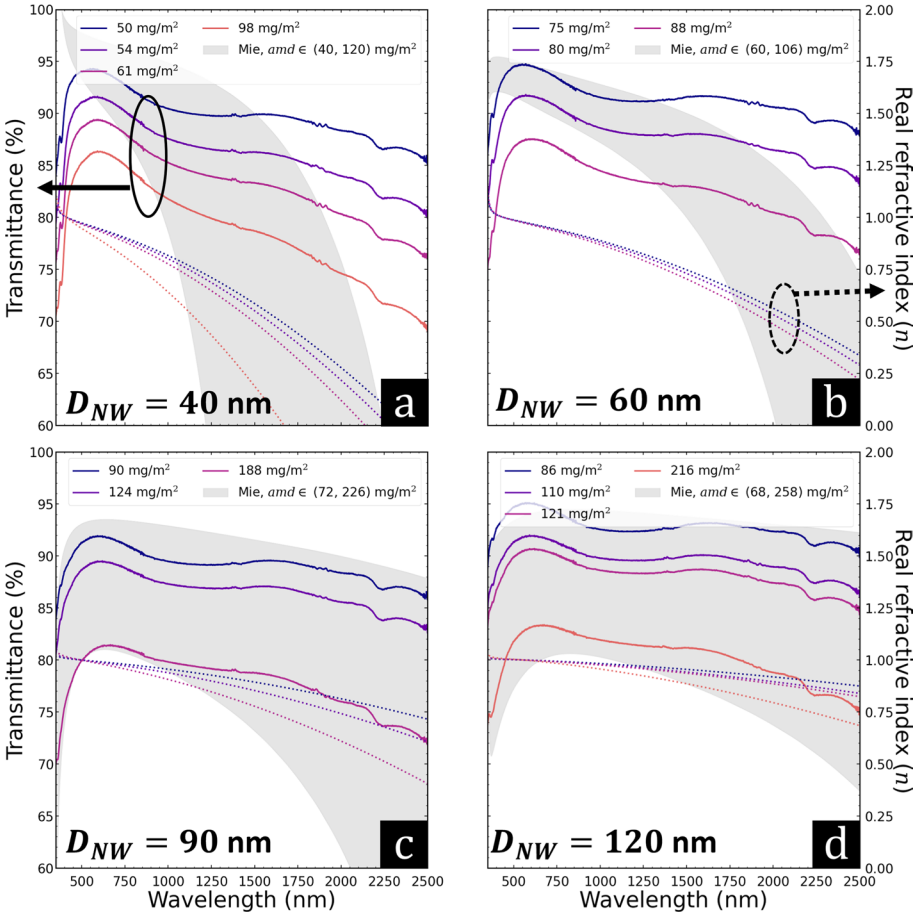

Fig. 4 *(Left axes)* Measured (solid lines) and predicted via the Mie+vdH models (gray area) transmittance in the visible and NIR spectra for samples of varying average D_{NW} (40 nm, 60 nm, 90 nm, 120 nm) and varying densities. The predicted results were calculated for *amd* values spanning the $(amd_{\min} - 20\%, amd_{\max} + 20\%)$ range for each given D_{NW}, such as to account for the intrinsic error associated to the *amd* measurement. *(Right axes)* Predicted real part of the RI, *n*, in dashed lines

films, where $n < 1$ typically rises with wavelength. This divergence underscores the hybrid nature of the nanowire network, necessitating consideration of its structural features to fully understand the observed physical trends. A key factor influencing this behavior is the average gap size between nanowires. As the ratio of the gap size to the incident wavelength grows, the optical response of the network increasingly resembles that of air rather than silver. Consequently, for shorter wavelengths, *n* approaches 1, the refractive index of air. Conversely, at longer wavelengths, the interaction between incident light and the network becomes more significant, causing *n* to deviate from 1 towards smaller values. This interpretation also explains the observed decrease in *n* with increasing areal mass density (*amd*). Denser networks, characterized by smaller gap sizes, exhibit more metallic-like optical properties, resulting in *n* values closer to those of a silver thin film [45]. Additionally, the relationship between nanowire diameter and gap size provides further insight: as the diameter increases, the average gap size grows due to the reduced number of nanowires required to achieve the same areal density [39]. Thicker nanowires, associated with larger gaps, exhibit optical behavior closer to air, as reflected by *n* values approaching 1 and a slower decline with increasing wavelength. These results highlight the nuanced interplay between the structural parameters of

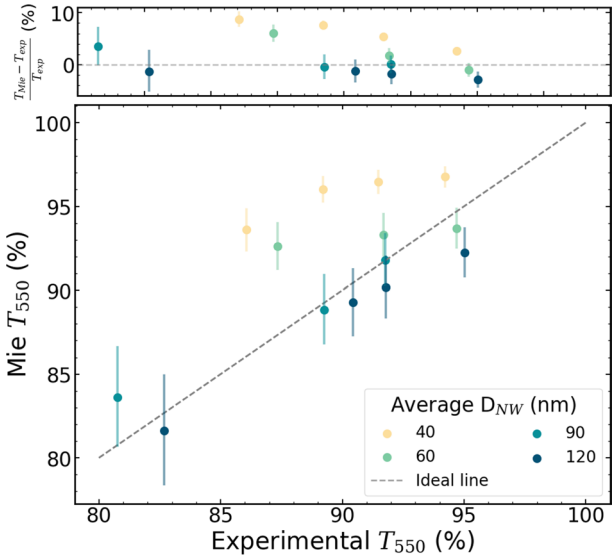

Fig. 5 Comparison between T_{550}, experimentally measured (dashed line) and theoretically predicted (symbols) by the Mie+vdH models, for AgNW networks of varying average diameters D_{NW}. The top graph shows the relative error between the predictions and the empirical data

nanowire networks and their refractive index behavior, emphasizing the importance of both density and nanowire diameter in the shaping of their optical properties.

On a final note, the results obtained in this study for the refractive index can be considered from the perspective of their application in optical simulations. Figure 5 illustrates the excellent agreement between the measured and predicted transmittance at $\lambda = 550$ nm (T_{550}), a standard metric for characterizing the optical properties of AgNW networks. The relative error across all datapoints remains below 10%, with accuracy improving as the nanowire diameter increases, consistent with the trends observed in Fig. 4. This strong correlation validates the use of our results as a reliable tool for the design of multilayer stacks incorporating AgNW networks. The ability to accurately predict the optical properties of these networks enables precise fine-tuning of their behavior, offering significant potential for the design of advanced optical applications.

4 Conclusion

In summary, through the use of a comprehensive theoretical approach, we have predicted the refractive indices and optical transmittance of AgNW networks from the visible to the NIR spectra. By combining Mie's scattering theory, van de Hulst's mixing model and Fresnel's equations, we achieve a predictive framework validated by experimental data. The model provides theoretical insights into the optical behavior of AgNW networks across the visible and NIR spectra, offering practical guidelines for optimizing these materials for diverse multimaterial applications. Our results also originally evidence the non-trivial, hybrid optical behavior of AgNW networks, which cannot be understood solely by looking at the silver response, but rather by having to consider explicitly the composite nature of the material, which introduces effective medium effects. We identified clear limitations to the use of these combined models, i.e. that the criterion λ/D_{NW} should be lower than 25 (size parameter $\alpha < 0.06$) due to key approximations of the van de Hulst mixing model. Future work could focus on extending this methodology to other heterogeneous TCMs including other metallic NW or carbon

nanotube networks [46], and on exploring the influence of environmental factors such as oxidation on optical performance. The integration of these models within device-level simulations, such as those using the Transfer Matrix Method, will further enhance their utility in designing advanced optoelectronic systems.

Supplementary Information

The online version contains supplementary material available at https://doi.org/10.1186/s11671-025-04312-9.

Supplementary file 1

Author contributions

A.B. conducted the research, prepared the figures, wrote the main manuscript and the supplementary information document. J.B. assisted in the experimental work. F.B. assisted in the methodology. F.R. and J.B. measured the transmittance and reflectance curves. B.Z. fabricated the samples. D.B. obtained funding for the research and helped in the methodology. N. D.N. obtained funding for the research, contributed to the methodology and managed the project. All authors reviewed the manuscript.

Funding

The authors gratefully acknowledge the financial support from the European Commission via the M-ERA. NET program (INSTEAD project). A. B. and N. D. N. acknowledge the financial support from F.R.S. - FNRS via the CDR project J.0157.24 and the PINT-MULTI project R.8012.20.

Data availability

All the relevant data are available within the paper and its Supporting Information file or from the corresponding author (Amaury Baret) upon reasonable request.

Declarations

Ethics approval and consent to participate

not applicable.

Competing interests

The authors have no competing interests to declare.

Received: 17 March 2025 / Accepted: 10 July 2025

Published online: 08 August 2025

References

1. Ellmer K. Past achievements and future challenges in the development of optically transparent electrodes. Nature Photon. 2012;6(12):809–17. https://doi.org/10.1038/nphoton.2012.282.
2. Nguyen VH, Papanastasiou DT, Resende J, Bardet L, Sannicolo T, Jiménez C, Muñoz-Rojas D, Nguyen ND, Bellet D. Advances in flexible metallic transparent electrodes. Small. 2022;18(19):2106006. https://doi.org/10.1002/smll.202106006.
3. Minami T. Transparent conducting oxide semiconductors for transparent electrodes. Semicond Sci Technol. 2005;20(4):35. https://doi.org/10.1088/0268-1242/20/4/004.
4. Lokanc M, Eggert R, Redlinger M. The availability of indium: the present, medium term, and long term. Technical Report NREL/SR–6A20-62409, 1327212 (October 2015). https://doi.org/10.2172/1327212
5. Sannicolo T, Lagrange M, Cabos A, Celle C, Simonato J-P, Bellet D. Metallic nanowire-based transparent electrodes for next generation flexible devices: a review. Small. 2016;12(44):6052–75. https://doi.org/10.1002/smll.201602581.
6. Kim D-J, Shin H-I, Ko E-H, Kim K-H, Kim T-W, Kim H-K. Roll-to-roll slot-die coating of 400 mm wide, flexible, transparent Ag nanowire films for flexible touch screen panels. Sci Rep. 2016;6(1):34322. https://doi.org/10.1038/srep34322.
7. Sekkat A, Sanchez-Velasquez C, Bardet L, Weber M, Jiménez C, Bellet D, Muñoz-Rojas D, Nguyen VH. Towards enhanced transparent conductive nanocomposites based on metallic nanowire networks coated with metal oxides: A brief review. J Mater Chem A. 2024;12(38):25600–21. https://doi.org/10.1039/D4TA05370B.
8. Bardet L, Roussel H, Saroglia S, Akbari M, Muñoz-Rojas D, Jiménez C, Denneulin A, Bellet D. Exploring the degradation of silver nanowire networks under thermal stress by coupling in situ X-ray diffraction and electrical resistance measurements. Nanoscale. 2024;16(2):564–79. https://doi.org/10.1039/D3NR02663A.
9. Khan A, Nguyen VH, Muñoz-Rojas D, Aghazadehchors S, Jiménez C, Nguyen ND, Bellet D. Stability enhancement of silver nanowire networks with conformal ZnO coatings deposited by atmospheric pressure spatial atomic layer deposition. ACS Appl Mater Interfaces. 2018;10(22):19208–17. https://doi.org/10.1021/acsami.8b03079.
10. Balty F, Baret A, Silhanek A, Nguyen ND. Insight into the morphological instability of metallic nanowires under thermal stress. J Colloid Interface Sci. 2024;673:574–82. https://doi.org/10.1016/j.jcis.2024.06.074.
11. Sannicolo T, Muñoz-Rojas D, Nguyen ND, Moreau S, Celle C, Simonato J-P, Bréchet Y, Bellet D. Direct imaging of the onset of electrical conduction in silver nanowire networks by infrared thermography: evidence of geometrical quantized percolation. Nano Lett. 2016;16(11):7046–53. https://doi.org/10.1021/acs.nanolett.6b03270.
12. Langley DP, Lagrange M, Nguyen ND, Bellet D. Percolation in networks of 1-dimensional objects: comparison between Monte Carlo simulations and experimental observations. Nanoscale Horiz. 2018;3(5):545–50. https://doi.org/10.1039/C8NH00066B.

13. Baret A, Bardet L, Oser D, Langley DP, Balty F, Bellet D, Nguyen ND. Bridge percolation: Electrical connectivity of discontinued conducting slabs by metallic nanowires. Nanoscale. 2024. https://doi.org/10.1039/D3NR05850F.
14. Pike GE, Seager CH. Percolation and conductivity: a computer study. I Phys Rev B. 1974;10(4):1421–34. https://doi.org/10.1103/PhysRevB.10.1421.
15. Žeželj M, Stanković I. From percolating to dense random stick networks: Conductivity model investigation. Phys Rev B. 2012;86(13): 134202. https://doi.org/10.1103/PhysRevB.86.134202.
16. Lagrange M, Langley DP, Giusti G, Jiménez C, Bréchet Y, Bellet D. Optimization of silver nanowire-based transparent electrodes: effects of density, size and thermal annealing. Nanoscale. 2015;7(41):17410–23. https://doi.org/10.1039/C5NR04084A.
17. Haacke G. New figure of merit for transparent conductors. J Appl Phys. 1976;47(9):4086–9. https://doi.org/10.1063/1.323240.
18. Ding Y, Cui Y, Liu X, Liu G, Shan F. Welded silver nanowire networks as high-performance transparent conductive electrodes: Welding techniques and device applications. Appl Mater Today. 2020;20: 100634. https://doi.org/10.1016/j.apmt.2020.100634.
19. Knittl Z. Optics of Thin Films; an Optical Multilayer Theory. Wiley Series in Pure and Applied Optics. Wiley, London (1976)
20. Bethune DS. Optical harmonic generation and mixing in multilayer media: analysis using optical transfer matrix techniques. J Opt Soc Am B JOSAB. 1989;6(5):910–6. https://doi.org/10.1364/JOSAB.6.000910.
21. Troparevsky MC, Sabau AS, Lupini AR, Zhang Z. Transfer-matrix formalism for the calculation of optical response in multilayer systems: from coherent to incoherent interference. Opt Express OE. 2010;18(24):24715–21. https://doi.org/10.1364/OE.18.024715.
22. Baret A, Khan A, Rougier A, Bellet D, Nguyen ND. Low-emissivity fine-tuning of efficient VO 2 -based thermochromic stacks with silver nanowire networks. RSC Appl Interfaces. 2025;2:94–103.
23. Zhao LL, Miao L, Liu CY, Wang HL, Tanemura S, Sun LX, Gao X, Zhou JH. Enhanced thermochromic properties and solar-heat shielding Ability of W x V1–x O2 thin films with ag nanowires capping layers. J Nanosci Nanotechnol. 2015;15(11):9192–6. https://doi.org/10.1166/jnn.2015.11423.
24. Yu X, Yu X, Zhang J, Chen L, Long Y, Zhang D. Optical constants of long silver nanowire thin films on glass calculated from the transmission spectra. Mater Lett. 2017;194:152–5. https://doi.org/10.1016/j.matlet.2017.02.044.
25. Abdel-Rahim RD, Nagiub AM, Pharghaly OA, Taher MA, Yousef ES, shaaban ER. Optical properties for flexible and transparent silver nanowires electrodes with different diameters. Opt Mater. 2021;117: 111123. https://doi.org/10.1016/j.optmat.2021.111123.
26. Tomiyama T, Yoshihara K, Yamazaki H. Polarization properties of silver nanowire/polymer composite films: diattenuation, retardance and depolarization. Opt Mater Express OME. 2019;9(6):2582–94. https://doi.org/10.1364/OME.9.002582.
27. Zhang J, Zhu X, Xu J, Xu R, Yang H, Kan C. Comparative study on preparation methods for transparent conductive films based on silver nanowires. Molecules. 2022;27(24):8907. https://doi.org/10.3390/molecules27248907.
28. Meyzonnette J-L, Mangin J, Cathelinaud M. Refractive index of optical materials. In: Musgraves JD, Hu J, Calvez L, editors. Springer handbook of glass. Cham: Springer; 2019. p. 997–1045. https://doi.org/10.1007/978-3-319-93728-1_29.
29. El-Zaiat SY. Determination of the complex refractive index of a thick slab material from its spectral reflectance and transmittance at normal incidence. Optik. 2013;124(2):157–61. https://doi.org/10.1016/j.ijleo.2011.11.039.
30. Bedia A, Bedia FZ, Aillerie M, Maloufi N, Benyoucef B. Influence of the thickness on optical properties of sprayed zno hole-blocking layers dedicated to inverted organic solar cells. Energy Procedia. 2014;50:603–9. https://doi.org/10.1016/j.egypro.2014.06.074.
31. Shalabney A, Lakhtakia A, Abdulhalim I, Lahav A, Patzig C, Hazek I, Karabchevsky A, Rauschenbach B, Zhang F, Xu J. Surface plasmon resonance from metallic columnar thin films. Photonics Nanostruct Fundam Appl. 2009;7(4):176–85. https://doi.org/10.1016/j.photonics.2009.03.003.
32. Manning HG, da Rocha CG, Callaghan CO, Ferreira MS, Boland JJ. The electro-optical performance of silver nanowire networks. Sci Rep. 2019;9(1):11550. https://doi.org/10.1038/s41598-019-47777-2.
33. Hamans RF, Parente M, Garcia-Etxarri A, Baldi A. Optical properties of colloidal silver nanowires. J Phys Chem C. 2022;126(20):8703–9. https://doi.org/10.1021/acs.jpcc.2c01251.
34. Khanarian G, Joo J, Liu X-Q, Eastman P, Werner D, O'Connell K, Trefonas P. The optical and electrical properties of silver nanowire mesh films. J Appl Phys. 2013;114(2): 024302. https://doi.org/10.1063/1.4812390.
35. Zhu Y, Kim S, Ma X, Byrley P, Yu N, Liu Q, Sun X, Xu D, Peng S, Hartel MC, Zhang S, Jucaud V, Dokmeci MR, Khademhosseini A, Yan R. Ultrathin-shell epitaxial Ag@Au core-shell nanowires for high-performance and chemically-stable electronic, optical, and mechanical devices. Nano Res. 2021;14(11):4294–303. https://doi.org/10.1007/s12274-021-3718-z.
36. Ma X, Zhu Y, Kim S, Liu Q, Byrley P, Wei Y, Zhang J, Jiang K, Fan S, Yan R, Liu M. Sharp-Tip silver nanowires mounted on cantilevers for high-aspect-ratio high-resolution imaging. Nano Lett. 2016;16(11):6896–902. https://doi.org/10.1021/acs.nanolett.6b02802.
37. Kerker M. The scattering of light and other electromagnetic radiation. New York: Elsevier; 2016.
38. Hulst HC. Light scattering by small particles. New York: Courier Corporation; 1981.
39. Atkinson J, Goldthorpe IA. Near-infrared properties of silver nanowire networks. Nanotechnology. 2020;31(36): 365201. https://doi.org/10.1088/1361-6528/ab94de.
40. Born M, Wolf E, Bhatia AB. Principles of optics: electromagnetic theory of propagation. Interference and diffraction of light. Cambridge: Cambridge University Press; 1999.
41. Nilsson PO, Lindau I, Hagström S. Optical plasma-resonance absorption in thin films of silver and some silver alloys. Phys Rev B. 1970;1(2):498–505. https://doi.org/10.1103/PhysRevB.1.498.
42. Liu P, Shi Z, Teng D, Liu F, Cao Y, Lin Y, Yang Z, Yang A, Zheng Y, Chen L. Optical characteristics of silver thin films from island to percolation in the ultra-wide infrared spectral range. Coatings. 2023;13(11):1910. https://doi.org/10.3390/coatings13111910.
43. Mishcenko MI, Travis LD, Lacis AA. Scattering, Absorption, and Emission of Light by Small Particles
44. Liu C, Jonas PR, Saunders C. Accuracy of the anomalous diffraction approximation to light scattering by column-like ice crystals. Atmos Res. 1996;41(1):63–9. https://doi.org/10.1016/0169-8095(95)00041-0.
45. Ciesielski A, Skowronski L, Trzcinski M, Szoplik T. Controlling the optical parameters of self-assembled silver films with wetting layers and annealing. Appl Surf Sci. 2017;421:349–56. https://doi.org/10.1016/j.apsusc.2017.01.039.

46. Ma X, Liu Q, Yu N, Xu D, Kim S, Liu Z, Jiang K, Wong BM, Yan R, Liu M. 6 nm super-resolution optical transmission and scattering spectroscopic imaging of carbon nanotubes using a nanometer-scale white light source. Nat Commun. 2021;12(1):6868. https://doi.org/10.1038/s41467-021-27216-5.

Publisher's Note